

## Lithosphere density model in Italy: no hint for slab pull

Brandmayr Enrico,<sup>1</sup> Marson Iginio,<sup>2,3</sup> Romanelli Fabio<sup>1,4</sup> and Panza Giuliano Francesco<sup>1,4</sup><sup>1</sup>Department of Geosciences, University of Trieste, Via Weiss 4, 34127, Trieste, Italy; <sup>2</sup>Department of Civil Engineering and Architecture, University of Trieste, P.le Europa 1, 34127, Trieste, Italy; <sup>3</sup>Istituto Nazionale di Oceanografia e di Geofisica Sperimentale, OGS, Borgo Grotta Gigante 42/C, 34010 Sgonico (TS), Italy; <sup>4</sup>The Abdus Salam International Centre for Theoretical Physics, Strada Costiera 11, 34014 Trieste, Italy

## ABSTRACT

The lithosphere–asthenosphere system of the Italic region in terms of shear-velocity and density distribution with depth is suitable to investigate the geodynamic context of the region. The velocity structure is obtained through nonlinear inversion of dispersion curves compiled from surface wave tomography on cells  $1^\circ \times 1^\circ$  and a smoothing optimization method to choose the representative cellular model, whose layering is used as fixed (*a priori*) information to obtain a density model by means of linear inversion of gravimetric data. Seismicity and heat flow are used as independent constraints in outlining both

the crustal and the seismic lid thickness; the nonlinear moment tensor inversion of recent damaging earthquakes allows some insight in the ongoing kinematic processes. Asymmetry between west-directed (Apennines) and east-directed (Alps, Dinarides) subductions is a robust feature of the velocity model, while density model reveals that slabs are not denser than the ambient mantle, thus supplies no evidence for slab pull.

Terra Nova, 00, 1–8, 2011

## Introduction

A pioneering work in density modelling of the upper mantle in the Italic region was performed by Marson *et al.* (1995) along transects around the Tyrrhenian rim, constructed within the geometrical constraints imposed by the results of the interpretation of aeromagnetic, seismic and seismological data. The advantage of joining geophysical models with geological and petrological data in order to understand the complex evolution of Italic region has been later discussed in Panza *et al.* (2007a): the study describes, for the first time, a very shallow crust–mantle transition and a very low S-wave velocity ( $V_S$ ) just below it, in correspondence of the submarine volcanic bodies (Magnaghi and Vavilov, Figs 1 and 2) indicating the presence of high amounts of magma. Panza *et al.* (2007b) integrated crustal geological and geophysical constraints with the  $V_S$  models along the TRANSMED III geotraverse. As a result, a new model of the mantle flow in a backarc setting, which reveals an easterly rising low-velocity zone (LVZ) in the active part of the Tyrrhenian basin, is obtained. An upper mantle circulation

in the Western Mediterranean, mostly easterly directed, affects the boundary between upper asthenosphere and lower asthenosphere, which undulates between about 180 and 280 km. An explanation for the detected shallow and very low velocity mantle in the

non-volcanic part of the Tyrrhenian region is presented in Frezzotti *et al.* (2009). These anomalous layers were generated by the melting of sediments and/or continental crust of the subducted Adriatic–Ionian (African) lid at temperatures above 1100 °C and

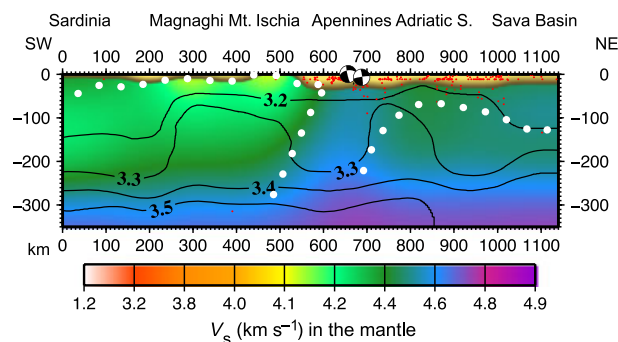


**Fig. 1** Sardinia–Balkans section:  $V_S$  and density model along a SW–NE profile from southern Sardinia to Sava Basin.  $V_S$  distribution is given by the color scale while continuous contour lines refer to density ( $\text{g cm}^{-3}$ ). Seismicity (red dots) and focal mechanisms of major events ('beach balls' plotted in map view) are shown as well. Dotted white lines delineate the lid-LVZ margin. Please refer to online version for interpretation of references to color. This profile samples the main geological and tectonic features of the central Mediterranean: (i) the southernmost part of the Corsica–Sardinia block characterized by scarce seismicity and rather low velocities in the lid, down to about 70 km of depth; (ii) the active part of Tyrrhenian basin, characterized by an asthenospheric LVZ emerging eastward from 70 km depth in the western part of the basin to 30 km depth below Ischia and well visible lithospheric 'boudinage'; (iii) the westward dipping Apennines, characterized by high seismicity even at intermediate depth and high velocities; (iv) a relatively low velocity and mostly aseismic lid beneath the Adriatic sea (as in section Adria42); (v) eastward dipping Dinaric slab, characterized by relatively high velocity and intermediate depth seismicity. Relatively low-density mantle is seen beneath Corsica–Sardinia block, Apennines and Dinarides, whereas a prominent positive density anomaly is found below Tyrrhenian and Adriatic seas.

Correspondence: Enrico Brandmayr, Department of Geosciences, University of Trieste, Via Weiss 4, 34127, Trieste, Italy. Tel: + 390405582128; fax: + 390405582111; e-mail: enrico.brandmayr@gmail.com

pressure greater than 4 GPa (130 km). The resulting low fractions of carbonate-rich melts have low density and viscosity and can migrate upward forming a carbonated partially molten CO<sub>2</sub>-rich mantle in the depth range from 130 to 60 km. Carbonate-rich melts upwelling to depth less than 60–70 km induce massive outgassing of CO<sub>2</sub>, that can migrate and be accumulated beneath the Moho and within the lower crust. Brandmayr *et al.* (2010) contributed to the debate on the geodynamical evolution of the Italic region with an improvement of the existing cellular model of the lithosphere–asthenosphere system of the area. The  $V_S$ -depth model considered in this work represents a further optimization of previous models constrained with independent studies concerning Moho depth (Dezes and Ziegler, 2001; Grad and Tiira, 2008; Tesauro *et al.*, 2008), seismicity–depth distribution (ISC, 2007) and P-wave velocity ( $V_P$ ) tomographic data (Pirromallo and Morelli, 2003). The layering of each representative cellular model is used as fixed (*a priori*) information to obtain a three-dimensional density model by means of linear inversion of gravimetric data (ISPRA, ENI and OGS, 2009). The results reveal some unexpected features of the mantle in subduction zones: in particular, no evidence of negative buoyancy of the subducting slabs with respect to the surrounding mantle is found. This finding agrees with recent xenolites studies (Kelly *et al.*, 2003) as well with the LLAMA model proposed by Anderson (2010). Therefore, the common concept of ‘slab pull’, usually evoked as leading force in subduction dynamics, but criticized in some detail by Doglioni *et al.* (2007), is hardly in agreement with our results.

## Methodology

A set of  $V_S$  models for cells sized 1° × 1° in the Italic region (Fig. 3), using the cellular dispersion curves compiled from surface wave tomography, has been obtained with the nonlinear ‘hedgehog’ inversion method (Panza *et al.*, 2007a,b), where  $V_P$  is a dependent parameter with respect to  $V_S$  (in general  $V_P/V_S = 3^{1/2}$ ) while density is fixed at popular values increasing with depth. These

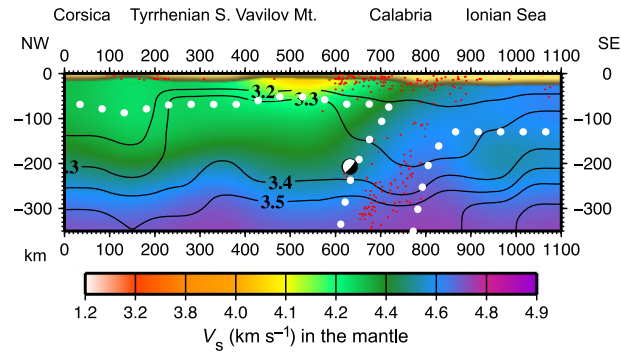


**Fig. 2** Tyrrhenian II section:  $V_S$  and density model along a NW–SE profile from southern Corsica to Ionian Sea. The labelling is the same as Fig. 1. Prominent feature of the section is the high velocity body representing subducting lid beneath Calabrian Arc, seismically active at all depths. To the west, the active part of the Tyrrhenian is marked by a lid at about 60–70 km thick, with some very low velocity soft mantle lid beneath volcanic areas. Lid is slightly thicker beneath Sardinia–Corsica block and reaches about 90 km of thickness. To the east of the Calabrian Arc, the Ionian lid is about 130 km thick, and the underlying mantle is relatively faster than the Tyrrhenian one. Generally, the mantle velocity is higher in the Ionian plate than in the Tyrrhenian basin. A prominent negative density anomaly characterizes the subducting slab and the Sardinia–Corsica block, whereas a positive anomaly characterizes both the active Tyrrhenian, with a 3.3 g cm<sup>-3</sup> density of about 60–70 km of depth, and the Ionian mantle, with a 3.3 g cm<sup>-3</sup> density reaching about 80 km of depth and a 3.4 g cm<sup>-3</sup> density at about 170 km of depth.

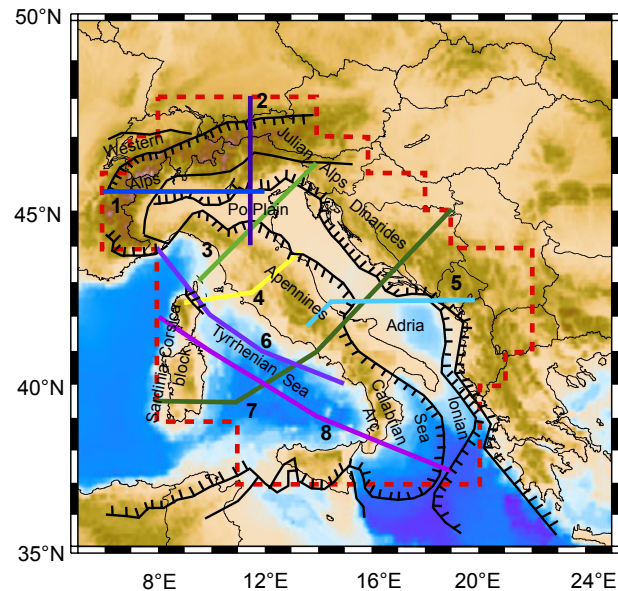


**Fig. 3** Study area: Map of the studied area, showing the geographical location of the considered sections, is enclosed by the dashed bold line. The cellular grid is omitted for sake of clarity. Main tectonic lineaments are shown, comb lines indicating compressive fronts and single lines indicating transfer zones. The sections are numbered as follows: (1) Ecos (Fig. 6); (2) Transalp (Fig. 9); (3) Adria43–46 (Fig. 7); (4) Crop03 (Fig. 10); (5) Adria42 (Fig. 8); (6) Tyrrhenian I (Fig. 5); (7) Sardinia–Balkans (Fig. 1); (8) Tyrrhenian II (Fig. 2).

cellular models extend to about 350 km of depth. In order to select the representative solution among this

set, all the solutions for each cell have been simultaneously processed with an optimized smoothing method with

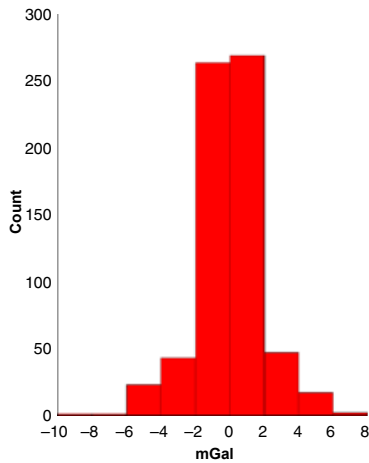


**Fig. 4** Density model uncertainties: Histogram of the differences between observed and model predicted gravimetric anomalies. The maximum value is 8 mGal, consistent with the quality and the noise level of the data.

the aim to define a smooth three-dimensional model of the lithosphere–asthenosphere system. The optimization method, that according to the Smoothness and Flatness criteria helps to choose, for each cell, as representative solution the one that minimizes the local lateral velocity gradient, consists of three algorithms: LSO (Local Smoothness Optimization) technique, that searches iteratively within five neighbour cells the solution for which the lateral gradient in shear wave velocity is minimized, GSO (Global Smoothness Optimization) and GFO (Global Flatness Optimization), which, respectively, search for the minimizing solution along a row of cells and through the whole study area. The three optimization algorithms (Boyadzhiev *et al.*, 2008; Brandmayr *et al.*, 2010) have been applied hierarchically, i.e. common solutions to LSO and GSO methods are fixed and then GFO is applied.

The resulting representative cellular models are appraised and constrained using independent studies concerning Moho depth (Dezes and Ziegler, 2001; Grad and Tiira, 2008; Tesauro *et al.*, 2008), seismicity–depth distribution (ISC, 2007),  $V_P$  tomographic data (Piromallo and Morelli, 2003) and other independent information as heat flow (Hurting *et al.*, 1991; Della Vedova *et al.*, 2001). The data from

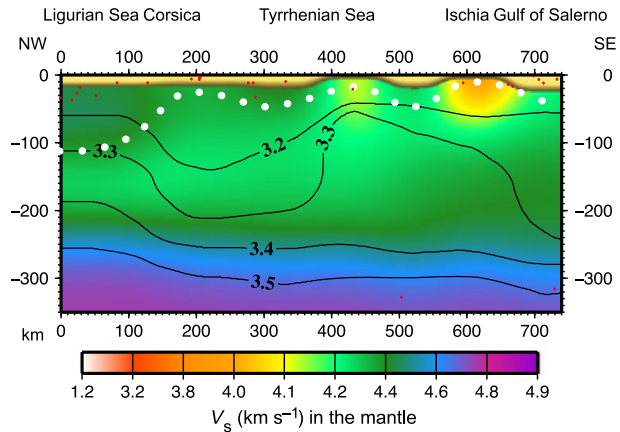


**Fig. 5** Tyrrhenian I section:  $V_S$  and density model along a NW–SE profile from Ligurian Sea to Gulf of Salerno. The labelling is the same as Fig. 1. This profile samples the Tyrrhenian Sea along its supposed direction of opening. It is clearly characterized by a south-eastward emerging LVZ from about 100 km of depth beneath Ligurian Sea and northern Corsica to about 30 km in the Ischia volcanic zone. The  $V_S$  model, the seismicity distribution and the so inferred lid–LVZ boundary fairly agree with extensive ‘boudinage’, at different scales (Ramsay and Huber, 1983, and references therein) that characterized the evolution of the basin still going on in present days. The northern part of the basin is characterized by relatively low-density mantle, in contrast with the southern active part, where density increases, as seen in other sections. Again, a relatively low density mantle is found east of Ischia, in the vicinity of Apennines subduction.

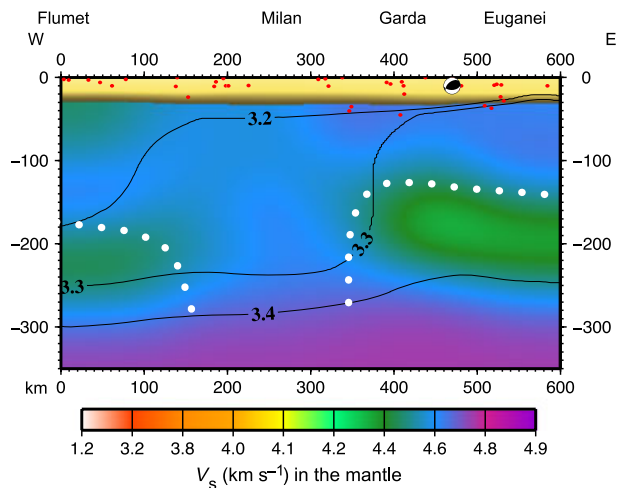


**Fig. 6** Ecors section:  $V_S$  and density model along a W–E profile from Flumet (western Alps) to Euganei Hills. The labelling is the same as Fig. 1. Striking feature of the section is the subduction of the European plate below the Adriatic plate, with deep ‘lithospheric roots’ below Milan, represented by high-velocity lid, well in agreement with what was shown by Mueller and Panza (1986). In contrast to Apennines subduction, no intermediate depth seismicity is observed in western Alps. To the West the LVZ is found at a depth of about 180 km. To the East, a prominent LVZ marks the Euganei Hills magmatic zone below a depth of about 130 km. The subducting lid is characterized by negative density anomaly, whereas a positive density anomaly is seen beneath Euganei Hills, as shallow as 30 km.

Dezes and Ziegler (2001), Tesauro *et al.* (2008) and Grad and Tiira (2008) are used to appraise the range

of Moho depth for each cell, by comparing it to the Moho depth, taken with its uncertainties, of the selected

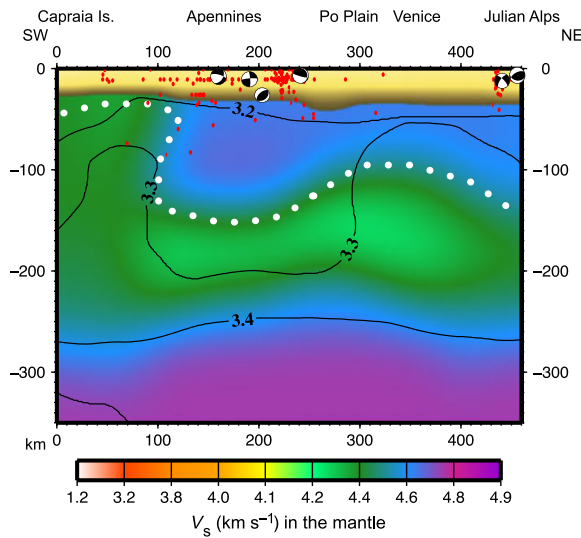


**Fig. 7** Adria43-46 section:  $V_S$  and density model along a SW–NE profile from Capraia Island to Julian Alps. The labelling is the same as Fig. 1. The pronounced high-velocity, almost vertical, slab represents Apennines subduction consistent with significant seismicity at intermediate depth. To the West, a low-velocity asthenospheric mantle wedge, mainly aseismic, is present. To the East, a high velocity lid about 100 km thick extends towards the NE-dipping Alpine subduction, marked by the shallow to intermediate depth seismicity in the right part of the section. The bottom of the lid is well marked by a LVZ. Striking features of density model are the negative density anomaly beneath Apennines and Julian Alps, with the exception of the relatively high-density value found beneath Tuscany, probably related to mantle wedge. Po plain and Northern Adriatic are instead characterized by relatively high-density mantle at depths ranging from 60 to 200 km.

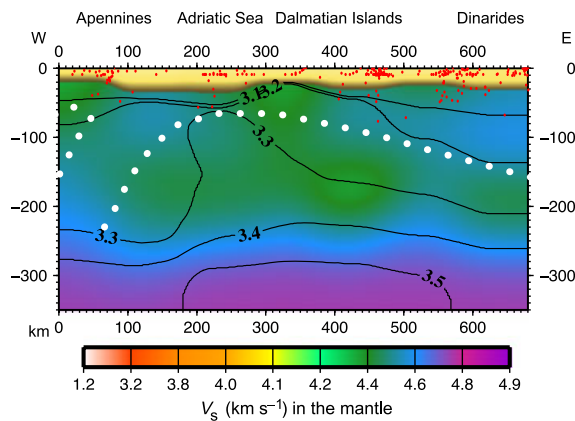


**Fig. 8** Adria42 section:  $V_S$  and density model along a W–E profile from central Apennines to Dinarides. The labelling is the same as Fig. 1. In this section, as in section Crop03, Apennines slab is marked by a high velocity almost vertical body, with some intermediate depth seismicity reaching about 60 km of depth. To the West, the low velocity at a depth of about 50–100 km, just above the sinking slab, is probably related to mantle wedge dynamics (e.g. dehydration). To the east, a relative low velocity, mainly aseismic, mantle lid extends for about 100 km just beneath the Adriatic crust. In the easternmost portion of the section, an eastward thickening lid is well marked by high velocity and intense intermediate depth seismicity, in fair agreement with a low angle Dinaric slab. Prominent negative density anomalies characterize both the Apennines and Dinarides at depth between 100 and 200 km, whereas high-density material seems to be related to the Adriatic plate, both in the lid and in the asthenospheric LVZ.

model. The depth distribution of seismicity is used as an additional criterion in outlining both Moho depth and lid thickness. The revised ISC (2007) catalogue for the period 1904–June 2005 is used and for each cell several histograms are computed, grouping hypocentres in depth intervals consistent with hypocentre depth uncertainties, 4 km for crustal seismicity and 10 km for mantle seismicity (Panza and Raykova, 2008; Brandmayr *et al.*, 2010). The analysis of focal mechanisms is a complementary information with respect to seismicity-depth distribution, even if statistically poorer than the latest, and it allows some insight in the kinematic processes acting in different tectonic provinces providing further constraints on the current geometries and stress field of the study region. Therefore, the dataset of the seismic moment tensor for the earthquakes with  $M_w \geq 4.8$  in the Italian region (Guidarelli and Panza, 2006; Brandmayr *et al.*, 2010), obtained using an advanced waveform inversion technique named INPAR (Sileny *et al.*, 1992; Sileny, 1998), has been updated to the most recent events.

The  $V_P$  data are taken from Piroallo and Morelli (2003), who provide a P-wave tomography study well resolving the upper mantle properties of the whole Mediterranean region. The calculated  $V_P$  value for each layer in our cellular models is used to reduce the uncertainty ranges of  $V_S$ , as far as the  $V_P/V_S$  ratio in the mantle is kept as close as possible to 1.82 (Kennett *et al.*, 1995).

The layering of each representative cellular model is used here as fixed (*a priori*) information to obtain a three-dimensional density model by means of linear inversion of gravimetric data. The starting density model is an upgrading of that given by Farina (2006) along a set of two-dimensional profiles in the Italic region and surroundings. We use the inversion software GRAV3D developed by the University of British Columbia-Geophysical Inversion facility (Li and Oldenburg, 1998). The inverse problem is formulated as an optimization problem where the following objective function of the density model is minimized, subject to the constraints that the data is reproduced within a given error tolerance:

$$\begin{aligned} \phi_m(\rho) = & \alpha_s \int_V w_s w^2(z) (\rho - \rho_0)^2 dv \\ & + \alpha_x \int_V w_x \left( \frac{\partial w(z) (\rho - \rho_0)}{\partial x} \right)^2 dv \\ & + \alpha_y \int_V w_y \left( \frac{\partial w(z) (\rho - \rho_0)}{\partial y} \right)^2 dv \\ & + \alpha_z \int_V w_z \left( \frac{\partial w(z) (\rho - \rho_0)}{\partial z} \right)^2 dv, \end{aligned} \quad (1)$$

where the functions  $w_s$ ,  $w_x$ ,  $w_y$  and  $w_z$  are spatially dependent, whereas  $\alpha_s$ ,  $\alpha_x$ ,  $\alpha_y$  and  $\alpha_z$  are coefficients which affect the relative importance of the different components of the objective function. The greater the ratio  $\alpha_x/\alpha_s$  the smoother the recovered model is along that axis direction. The objective function defined by Eq. (1) has the flexibility to allow many different models to be constructed. The relative closeness of the final model to the starting model at any location is controlled by the function  $w_s$ . The weighting functions  $w_x$ ,  $w_y$  and  $w_z$  can be designed to enhance or attenuate structures in various regions in the model domain. The function  $w(z)$  in Eq. (1) is a depth weighting that depends upon the model discretization and observation location. The weighting function is used to counteract the decay of the kernel function with depth. It is assumed that the data are contaminated by Gaussian noise with zero mean and, to define a measure of the misfit, a two-norm measure is used. The inverse problem is solved by finding a density that minimizes the measure and misfits the data according to the noise level. As the density contrast is limited to a small range for any practical problems, and often there are well-defined bounds on the density contrast based on other geological information, it is possible to impose constraints to restrict the solution to lie between a lower and upper bound. The data used for the inversion are a subset of those used to produce the Digital Gravity Maps of Italy (ISPRA, ENI and OGS, 2009). A Gaussian noise with amplitude of 1.5 mGal has been added to the gravity anomaly data. The input mesh consists of  $32 \times 22$  cells (each  $0.5^\circ \times 0.5^\circ$ ) along the  $x$  and  $y$  directions, where the density is defined vs. depth in 12 layers of different thickness, fixed on the base of the  $V_S$

layering. As the observed and inverted data are Bouguer anomalies, in the water layer, when present, the Bouguer density has been used and allowed to vary only within a very limited range of density ( $-0.01$ ,  $+0.01 \text{ g cm}^{-3}$ ), i.e. fixed for any practical reason. The differences between the observed and predicted anomaly values show a Gaussian behaviour with a standard deviation of 1.8 mGal, consistent with the quality and level of the noise (Fig. 4).

## Discussion

The lid and the LVZ are different concepts from the lithosphere and the asthenosphere (e.g. see p. 12 in Brandmayr *et al.*, 2010), although the terms are often confused in literature, as clearly evidenced by Anderson (2010). In the following discussion, we use the terms lid and LVZ when referring to strictly seismological features. Velocity features of most of the sections, discussed in detail in

Brandmayr *et al.* (2010), are substantially confirmed and can be summarized as follows: high velocity lid characterizes subducting slabs ( $V_S > 4.5 \text{ km s}^{-1}$ ); the bottom of the lid is generally marked by a velocity inversion, or at least by a null gradient, with  $V_S$  lower than  $4.4 \text{ km s}^{-1}$ ; very low mantle velocities (soft mantle lid,  $V_S$  even lower than  $3.6 \text{ km s}^{-1}$ ) are found in the active part of the Tyrrhenian basin (Figs 5, 1 and 2), in agreement with a high percentage of melts and magmas (Panza *et al.*, 2007a).

Asymmetry between west-directed (Apennines) and east-directed (Alps, Dinarides) subductions is a robust feature of the model: low angle subduction is seen in western Alps, along section Ecors (Fig. 6) and in Julian Alps and Dinarides (Figs 7, 8 and 1). Very low angle collision process ( $< 7^\circ$ ) is found in Eastern Alps, along section Transalp (Fig. 9). Subduction below Apennines (Fig. 10a) is steeper than below Alps and Dinarides in all analysed sections. This feature is

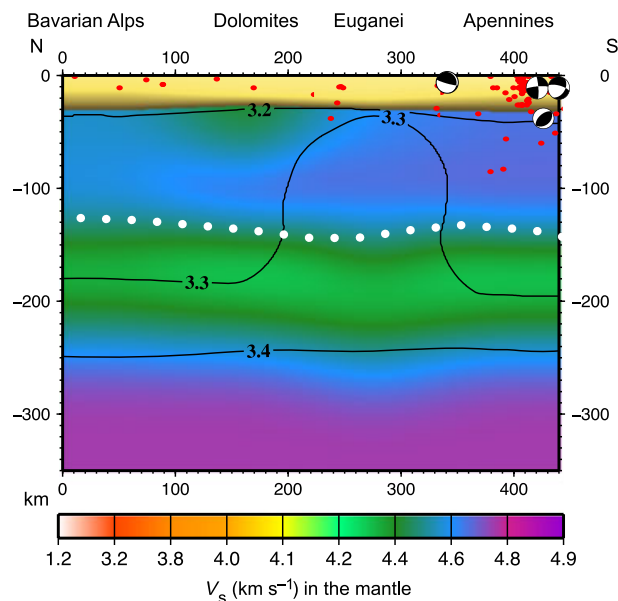


**Fig. 9** Transalp section:  $V_S$  and density model along an N–S profile from Bavarian Alps to Northern Apennines. The labelling is the same as Fig. 1. The low-angle subduction of the European plate below the Adriatic plate is fairly well evidenced by gently N–S dipping high-velocity lid and in accordance with scarce shallow seismicity and almost absent intermediate depth seismicity, as seen in Ecors section. A relatively low velocity lid is found beneath Dolomites, just below the Moho. The bottom of the lid is found at about 120–140 km of depth and overlies a well-marked LVZ in the asthenosphere. In the southernmost part of the section, Apennines subduction is delineated by high seismicity that reaches intermediate depth. The prominent high-density body, as shallow as 40 km of depth, below Venetian plain, may be a signature of the Euganei Hills magmatic activity.

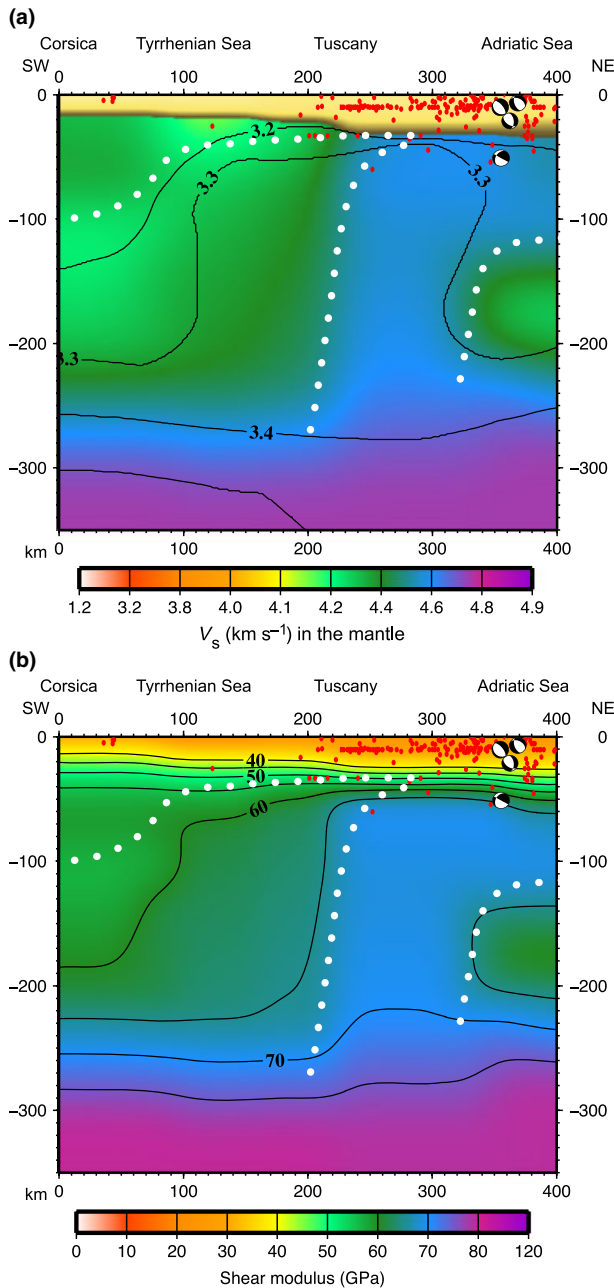


**Fig. 10** Crop03 section: (a)  $V_s$  and density model along a SW–NE profile from northern Corsica to Adriatic Sea. The labelling is the same as Fig. 1. The pronounced high-velocity, almost vertical, slab represents Apennines subduction. To the West, an asthenospheric LVZ emerging from about 100 km depth beneath Corsica to about 40 km depth beneath Tuscany clearly marks the bottom of the lid. To the East of the subduction, a high-velocity lid extends beneath Adria down to about 120 km of depth, lying on a well marked LVZ. A high density body is seen below Tuscany and in the subducting slab, whereas lower density characterizes both Corsica block and Adriatic mantle. (b) The shear modulus ( $\mu$ ), in GPa, along the same section, gives a more clear-cut picture of the subducting slab.

much more clear-cut in a section where the distribution of the shear modulus ( $\mu$ ) is shown (e.g. Fig. 10b); as a rule, in the Alpine and Adriatic

sections, the dotted white line corresponds to the isoline of 65 GPa. The asymmetric feature, as well the eastward emerging LVZ in the Tyrrhe-

nian asthenosphere (Fig. 5) is in agreement with an east-directed mantle flow (Doglioni *et al.*, 1999). In all the sections but one, the velocity in the mantle on the west side of Apennines is lower than in the east side, both in the Ionian plate and in the Adriatic plate, mainly in the depth range from 100 to 200 km (asthenosphere), where the eastward flow can reach its maximum. The exception is given by section Adria43-46 (Fig. 7), across northern Apennines, where a marked LVZ is found below and to the north-east of the slab ( $V_s$  about  $4.2 \text{ km s}^{-1}$ ), whereas mantle velocities on the western flank are about  $4.35 \text{ km s}^{-1}$ . Similarly, asymmetric features in the velocity model can be observed between northern and southern Tyrrhenian basin, with a longitudinal axis roughly corresponding to the  $41^\circ\text{N}$  parallel. The southern (active) part of the basin is generally characterized by mantle velocities that are lower than those in its northern part (Figs 5 and 2); this difference can be attributed to several causes, e.g. different extension rates, difference in the intensity of mantle flow, presence of lithospheric fragments, metamorphism and/or compositional differences.

In the density model, a dominant feature in all the sections is that the subducting slabs are not denser than the ambient mantle, but they are slightly lighter. This feature persists, regardless of the orientation or type (i.e. Alps or Apennines) of collision/subduction.

Western Alps (Fig. 6) and Sardinia–Corsica block (Fig. 1) present a common distribution of density with depth, with a relative low-density mantle with respect to surroundings ( $3.3 \text{ g cm}^{-3}$  at about 230–250 km). This similarity may be due to their common origin, as Sardinia–Corsica block is a fragment of the European Plate (Lustrino *et al.*, 2009 and references therein). On the contrary, a density higher than the surroundings is found in the LVZ, with the  $3.3 \text{ g cm}^{-3}$  density reaching depths of about 70 km (Figs 5, 1 and 2), in particular, in the active part of the Tyrrhenian basin, where the asthenosphere is very shallow. Similarly, high density mantle is found beneath Po Plain and northern Adriatic (Figs 9 and 7).

The north–south asymmetry observed in the mantle velocities of the Tyrrhenian basin persists in the density model, with lower mantle densities in the northern part of the basin than in the southern (Fig. 5), the axis of symmetry being the 41°N parallel. Therefore, higher densities in the mantle seem to be strictly related to the eastward flow itself and to its ascent beneath the back-arc basin.

All these findings suggest that material coming from a deep source, in spite of depressurisation, persists to be denser than ambient mantle. Therefore, the common concept of ‘slab pull’, usually evoked to be one of the leading forces in subduction dynamics, is hard to be endorsed in this context, as no evidence of negative buoyancy of the slab itself with respect to the ambient mantle is found.

## Conclusions

The asymmetry between E-verging and W-verging subduction zones, clearly evidenced by  $V_S$  model, supports the hypothesis of an eastward mantle flow, especially in the LVZ, between 120 and 200 km of depth, that is likely to represent the decoupling between the lithosphere and the underlying mantle at global scale (Panza *et al.*, 2010). The flow is very shallow in the active Tyrrhenian basin due to mantle compensation induced by the eastward migration of the Apennines subduction. High densities ( $> 3.3 \text{ g cm}^{-3}$ ) in the mantle seem to be strictly related to the eastward flow itself and to its ascent beneath the back-arc basin or to other extensional tectonics or to volcanism. On the contrary, slabs are not denser than the ambient mantle, but they appear to be slightly lighter; this evidence conflicts with the concept of ‘slab pull’ and thus calls for different actors in subduction dynamics (e.g. Doglioni *et al.*, 2007).

## Acknowledgements

We thank A. Levshin and Don L. Anderson for thoughtful and constructive reviews. This research has benefited of the grant ‘Studio della struttura della crosta e del mantello superiore dell’area mediterranea mediante metodologie sismologiche di inversione non lineare’ by Dipartimento

di Geoscienze dell’Università degli Studi di Trieste, funded by the Italian Ministero dell’Istruzione, dell’Università e della Ricerca PRIN 2008 and Italian PNRA (2004/2.7-2.8) ‘‘Sismologia a larga banda, struttura della litosfera e geodinamica nella regione del Mare di Scotia’’. This research has been partly developed in the framework of the ASI-Pilot Project ‘SISMA: SISMA-Information System for Monitoring and Alert’. Gravimetric Inversion is performed with the program Grav3D, developed by University of British Columbia (‘‘UBC’’), of 2075 Westbrook Mall, Vancouver, British Columbia V6T 1Z3 and licensed by UBC. Part of figures have been plotted using GMT (Generic Mapping Tools; Wessel and Smith, 1995).

## References

- Anderson, D.L., 2010. Hawaii, boundary layers and ambient mantle – geophysical constraints. *J. Petrol.*, doi: 10.1093/petrology/egq068.
- Boyadzhiev, G., Brandmayr, E., Pinat, T. and Panza, G.F., 2008. Optimization for non linear inverse problem. *Rendiconti Lincei Sci. Fis. e Nat.*, **19**, 17–43.
- Brandmayr, E., Raykova, R.B., Zuri, M., Romanelli, F., Doglioni, C. and Panza, G.F., 2010. The lithosphere in Italy: structure and seismicity. In: *The Geology of Italy: tectonics and life along plate margins* (M. Beltrando, A. Peccerillo, M. Mattei, S. Conticelli and C. Doglioni, eds), *J. Virtual Explorer* [online], **36**, 1, doi:10.3809/jvirtex.2010.00224.
- Della Vedova, B., Bellani, S., Pellis, G. and Squarci, P., 2001. Deep temperatures and surface heat flow distribution. In: *Anatomy of an Orogen* (G.B. Vai and I.P. Martini, eds), pp. 65–76. Kluwer Academic Publications, Dordrecht, The Netherlands.
- Dezes, P. and Ziegler, P., 2001. *Map of the European Moho*. 2nd EUCOR-URGENT Workshop (Upper Rhine Graben Evolution and Neotectonics), Mt. St. Odile, France.
- Doglioni, C., Gueguen, E., Harabaglia, P. and Mongelli, F., 1999. On the origin of west-directed subduction zones and application to the western Mediterranean. In: *The Mediterranean Basins: Tertiary Extension Within the Alpine Orogen* (B. Durand, L. Jolivet, F. Horváth and M. Séranne, eds), *Geol. Soc. London*, **156**, 541–561.
- Doglioni, C., Carminati, E., Cuffaro, M. and Scrocca, D., 2007. Subduction kinematics and dynamic constraints. *Earth-Sci. Rev.*, **83**, 125–175.
- Farina, B.M., 2006. *Lithosphere-asthenosphere system in Italy and surrounding areas: optimized non-linear inversion of surface-wave dispersion curves and modelling of gravity bouguer anomalies*. Doctoral dissertation, University of Trieste.
- Frezzotti, M.L., Peccerillo, A. and Panza, G.F., 2009. Carbonate metasomatism and CO<sub>2</sub> lithosphere-asthenosphere degassing beneath the Western Mediterranean: An integrated model arising from petrological and geophysical data. *Chem. Geol.*, **262**, 108–120.
- Grad, M. and Tiira, T., 2008. The Moho depth map of the European Plate. *Geophys. J. Int.*, **176**, 279–292.
- Guidarelli, M. and Panza, G.F., 2006. INPAR, CMT and RCMT seismic moment solutions compared for the strongest damaging events ( $M \geq 4.8$ ) occurred in the Italian region in the last decade. *Rendiconti Accademia Nazionale delle Scienze detta dei XL Memorie di Scienze Fisiche e Naturali*, **124**, XXX P. II, 81–98.
- Hurting, E., Cermak, V., Haenel, R. and Zui, V. (eds), 1991. *Geothermal Atlas of Europe*. Hermann Haack Verlag, Gotha, 156 pp.
- ISC (2007). Seismicity-depth distribution. International Seismological Centre, Available at: <http://www.isc.ac.uk>
- ISPRA, ENI and OGS, 2009. Cartografia Gravimetrica Digitale d’Italia alla scala 1:250.000.
- Kelly, R.K., Kelemen, P.B. and Jull, M., 2003. Buoyancy of the continental upper mantle. *Geochem. Geophys. Geosyst.*, **4**, 1017.
- Kennett, B.K.N., Engdahl, E.R. and Buland, R., 1995. Constraints on seismic velocities in the earth from travel times. *Geophys. J. Int.*, **122**, 108–124.
- Li, Y. and Oldenburg, D.W., 1998. 3D inversion of gravity data. *Geophysics*, **63**, 109–119.
- Lustrino, M., Morra, V., Fedele, L. and Franciosi, L., 2009. Beginning of the Apennine subduction system in central western Mediterranean: constraints from Cenozoic ‘‘orogenic’’ magmatic activity of Sardinia (Italy). *Tectonics*, **28**, TC5016.
- Marson, I., Panza, G.F. and Suhadolc, P., 1995. Crust and upper mantle models along the active Tyrrhenian rim. *Terra Nova*, **7**, 348–357.
- Mueller, S. and Panza, G.F., 1986. Evidence of a deep-reaching lithospheric root under the Alpine Arc. In: *The Origin of Arcs*, vol. **21** (F.C. Wezel, ed.), pp. 93–113. Elsevier, Amsterdam.
- Panza, G.F. and Raykova, R.B., 2008. Structure and rheology of lithosphere in Italy and surrounding. *Terra Nova*, **20**, 194–199.
- Panza, G.F., Peccerillo, A., Aoudia, A. and Farina, B.M., 2007a. Geophysical and petrological modelling of the structure and composition of the crust and upper mantle in complex geodynamic settings: the Tyrrhenian Sea and surroundings. *Earth-Sci. Rev.*, **80**, 1–46.

- Panza, G.F., Raykova, R.B., Carminati, E. and Doglioni, C., 2007b. Upper mantle flow in the western Mediterranean. *Earth Planet. Sci. Lett.*, **257**, 200–214.
- Panza, G.F., Doglioni, C. and Levshin, A., 2010. Asymmetric ocean basins. *Geology*, **38**, 59–62.
- Piromallo, C. and Morelli, A., 2003. P wave tomography of the mantle under the Alpine-Mediterranean area. *J. Geophys. Res.*, **108**, 2065–2088.
- Ramsay, J.G. and Huber, M.I., 1983. The techniques of modern structural Geology. In: *Volume 1: Strain analysis*, p. 307. London, Academic Press.
- Sileny, J., 1998. Earthquake source parameters and their confidence regions by a genetic algorithm with a “memory”. *Geophys. J. Int.*, **134**, 228–242.
- Sileny, J., Panza, G.F. and Campus, P., 1992. Waveform inversion for point source moment tensor retrieval with optimization of hypocentral depth and structural model. *Geophys. J. Int.*, **109**, 259–274.
- Tesauro, M., Kaban, M.K. and Cloetingh, S.A.P.L., 2008. EuCRUST-07: a new reference model for the European crust. *Geophys. Res. Lett.*, **35**, L05313.

*Received 8 May 2011; revised version accepted 17 June 2011*